Estimation of neutron kerma in biological tissue containing boron and gadolinium compounds for neutron capture therapy

I. Sheino[1], V. Khokhlov[1], V. Kulakov[1], K. Zaitsev[2]

[1]*SSC – Institute of Biophysics, Moscow*
[2]*Moscow Engineering Physics Institute (State University)*

Introduction

Neutron capture therapy (NCT) of malignant tumors currently uses compounds containing ^{10}B (enrichment >99%) and compounds with Gd in the natural mixture. The use of these drugs provides an essential increase of local energy release in the site of their distribution under neutron irradiation.

Materials and Methods

Energy release resulting from interactions of neutrons with the nuclei of substance is usually divided in two components:
1. local energy release from neutron reactions;
2. energy release from absorption of secondary photons originating as a result of these reactions.

Local energy release occurs due to the slowdown of charged particles - products of nuclear reactions (including recoil nuclei) on distances up to several tens microns. In this case the released energy is usually supposed to be absorbed in the location of its release.

The energy of secondary photons has a wide spectrum (from x-ray to gamma radiations with energy up to ~10 MeV). Their range before absorption in a tissue-equivalent medium can reach several tens centimeters.

Calculation of the absorbed dose in a target organ is determined by the sum of the doses of neutrons and secondary gamma, and the dose of primary photons of the beam. The values of the absorbed dose are usually approximated by kerma of separate radiation components.

Thus, the calculation of a dose requires:

- energy spectrum of neutrons and photons in the target organ;
- energy dependence of specific partial kerma of neutrons and photons for all elements in the composition of biological tissue and NCT drugs used.

Neutron kerma

For the calculation of kerma distribution for a known neutron spectrum in a point of space with the coordinate *r,* the following expression is used:

$$K(r,t) = k_D \int dE\, \Phi(r,E) \cdot \sum_i n_i(r,t) \sum_j \sigma_{ij}(E)\, \overline{E}_{ij}(E) / \rho(r) = \int dE\, \Phi(r,E) \cdot \sum_i w_i(r,t) \cdot k_i(E)\ ,\ \text{Gy/s}$$

where k_D=1.602 10^{-10} *Gy·g/MeV* — energy conversion factor from MeV to Gy×g, (obtained from the known ratio: 1 MeV=1.602 10^{-13} J); E – neutron energy, *MeV*; $\Phi(r,E)\,dE$ – neutron flux in the point *r* on the energy interval *dE*, *neutron/cm²/s*: n_i – atomic density of the *i*-th nuclide of the medium, *atom/cm³*; $\sigma_{ij}(E)$ –microscopic cross-section of reaction *j* at interaction of a neutron with energy *E* on the *i-th* nuclide of medium, *cm²/atom*; $\overline{E}_{ij}(E)$ - average energy released in reaction *j* at interaction of a neutron of energy *E* on the *i-th* nuclide of medium, *MeV*; $\rho(r)$ - mass density of medium, g*/cm³; $w_i(r,t)$*- relative mass fractions of nuclides in the medium, accounting for their distribution in time *t*; $k_i(E)$ – energy dependence of specific partial kerma of the *i-th* nuclide (kerma factor):

$$k_i(E) = k_D \cdot \frac{N_A}{A_i} \cdot \sum_j \sigma_{ij}(E) \cdot \bar{E}_{ij}(E), \qquad Gy \cdot cm^2/neutron.$$

N_A - Avogadro constant = 0.6023 10^{24} , *a.m.u./g* (*a.m.u.- atomic mass unit); A_i* – atomic mass of the nuclide, *a.m.u./atom*. Kerma factor can also be calculated by the energy balance method:

$$k_i(E) = k_D \cdot \frac{N_A}{A_i} \cdot \sum_j \sigma_{ij}(E) \cdot [E + Q_{ij} - Y_{\gamma ji} \bar{E}^{\gamma}_{ji}], \qquad Gy \cdot cm^2/neutron,$$

where $\sigma_{ij}(E)$ - cross-section of reaction *j* on the *i*-th material of the medium; Q_{ij} – energy of reaction *j* on the *i*-th material of the medium; $Y_{\gamma ji}(E)$, $\bar{E}_{\gamma ji}(E)$ - yield of secondary photons and their mean energy, respectively;

The energy balance method determines the energy of charged particles as the difference of the total energy of the reaction (defined by the Q-value) and the total energy of secondary photons generated in this reaction. The latter formula is derived assuming the absence of secondary neutrons.

Relative mass fractions of nuclides - w_i, included in biological tissues and drugs used in NCT, are shown in the table below.

Boron and gadolinium in NCT drugs produce secondary radiation of different nature in the tumor. Fig. 1 shows the schemes of nuclear reactions. Apparently, all secondary radiation of the reaction on ^{10}B is localized only in the place of its location. The range of decay products is 5 - 9 μm. In the reaction on ^{157}Gd there occurs rather hard photon radiation and electron radiation (conversion and Auger electrons). The latter, with a range of 1 - 40 μm, is localized in the location of gadolinium.

Data on specific partial kerma of neutrons used in the calculations were taken from J.T. Goorley et al. [1] available in the electronic database EPAPS, on the site http://ftp.aip.org/epaps/medical_phys/E-MPHYA6-29-009201/. The components of kerma in soft biological tissue are shown in the following figure.

Table 1.Composition of biological tissues and drugs for NCT (mass content of nuclides)

№	Element	Z	Tissue, Soft	Blood, Whole	Bone, Cortical	Brain, Grey/White Matter	BSH (enrichment in ^{10}B - 99%)	BPA-G (enrichment in ^{10}B - 99%)	Gd-DTPA basic substance of the drug Dipentast
1	H	1	0.102	0.102	0.034	0.107	0.0527	0.0572	0.03067
2	C	6	0.143	0.110	0.155	0.145		0.5113	0.28427
3	N	7	0.034	0.033	0.042	0.022		0.0397	0.07104
4	O	8	0.708	0.745	0.435	0.712		0.3632	0.27046
5	Na	11	0.002	0.001	0.001	0.002	0.2186		0.07772
6	Mg	12			0.002				
7	P	15	0.003	0.001	0.103	0.004			
8	S	16	0.003	0.002	0.003	0.002	0.1524		
9	Cl	17	0.002	0.003		0.003			
10	K	19	0.003	0.002		0.003			
11	Ca	20			0.225				
12	Fe	26		0.001					
13	**B**	**5**					0.5762	0.0284	
14	**Gd**	**64**							0.26584

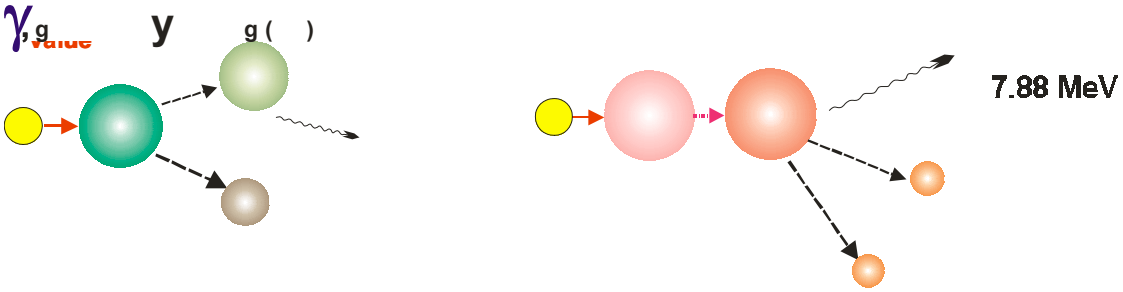

Fig. 1. Nuclear reactions in NCT.

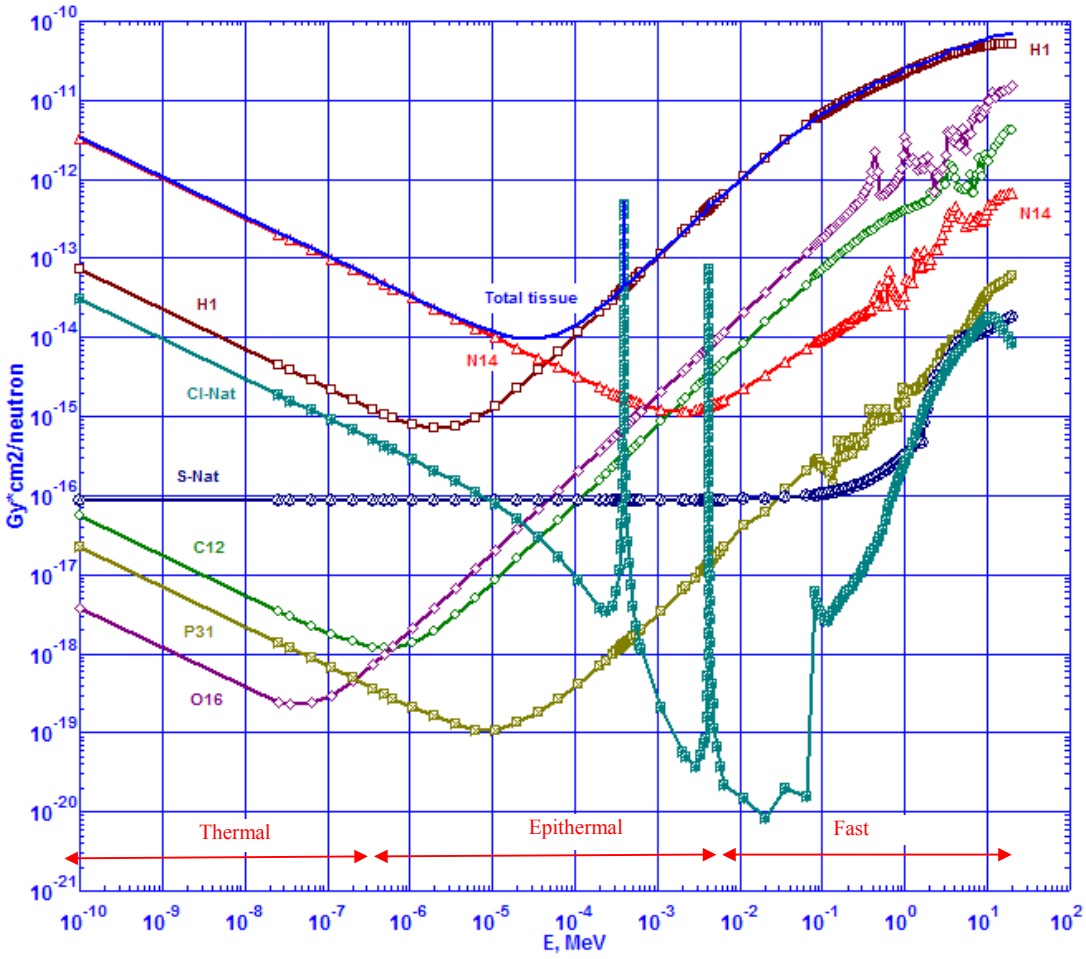

Fig. 2. Partial $w_i k_i(E)$ kerma of nuclides, and full kerma of biological tissue vs. neutron energy. (According to [1]).

The energy dependence of specific ^{10}B kerma calculated by the energy balance method is taken from the work by J.T. Goorley et al. [1].

For the first time we obtained the energy dependence of specific kerma for gadolinium in our researches. For this purpose, we carried out assessments of the spectrum of electrons and photons of the thermal neutron capture reaction ^{157}Gd(n,γ). The calculated values of the photon spectrum of this reaction obtained by J.Stepanek at al. [2], C Wang [3], *T. Goorley at al.* [4] on processing of the file ENSDF do not contain information on the photon emission over the range of 2.1 MeV to 3.7 MeV. The total energy of photons is ≈2.2 MeV, which is much lower than the excitation energy of ^{158}Gd (Q_{value} =7.94 MeV). The following table presents results of a comparative analysis of the calculated parameters of secondary particle spectra in this reaction.

Table 2.Comparison of the calculated parameters of the electron and photon spectra in the reaction $^{157}Gd(n,\gamma)$

Average value per reaction	*T.Goorley, H.Nikjoo, 2000 [4]*	*M.Rivard, J.Stepanek, 2000*	*C. K. Wang at all, 1999 [3]*	*G.Miller at al., 1993*	*J.Stepanek, 1997 [2]*	*Our estimations by the data of J.K.Tuli and J.Stepanek*	*S.A.Klykov et al. 2001.[7]*	*Y.Sakurai at al., 2002 [8]*
Yield of Auger electrons	4.93	9.71	6.7		4.8			
Energy of Auger electrons (keV)	4.19	4.14	4.80		3.94			
Yield of internal conversion electrons	0.69	0.649	0.725	0.732	0.647			
Energy of internal conversion electrons (keV)	45.9	45.51	65.91	91.00	45.39			
Total yield of electrons	5.62	10.36	7.42		5.45			
Total energy of electrons (keV)	50.1	49.65	70.7		49.33		65±15	63.5
Yield of x-rays	0.84	0.32			5.77	0.63		
Energy of x-rays (keV)	10.73	10.33			10.5	24.1		
Yield of γ-radiation	1.83	1.56		3.29	1.56	1.55		
Energy of γ-radiation (keV)	2437	2219		7871	2219	2206		
Total yield of photons	2.66	1.558			7.33	2.18		
Total energy of photons (keV)	2451	2229			2229	2230		

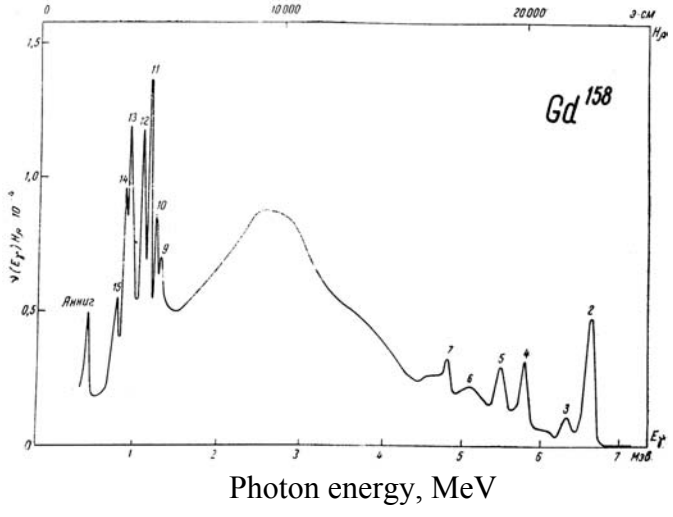

Fig. 3. Spectrum of γ-radiation at deexcitation of ^{158}Gd (the reaction $^{157}Gd(n,\gamma)^{158}Gd$ on thermal neutrons) [6]. The total photon energy ≈ 8 MeV

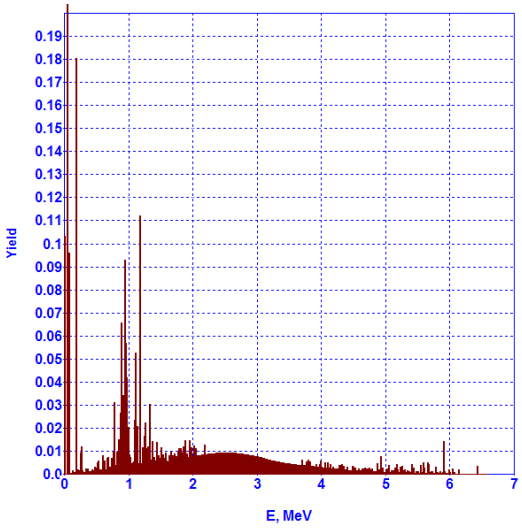

Fig. 4. Calculated photon spectrum (the reaction $^{157}Gd(n,\gamma)^{158}Gd$). The axis of ordinates is the number of photons in an interval of 10 keV. Total energy of photon spectrum E_γ= 7.87 MeV, Yield ≈4.

Our assessments of the photon spectrum are based on the results of J. K. Tuli [5] for the lines and data of L. Groshev at al. [6] (fig. 3) for the continuous part of the photon spectrum. Using these data in combination, for the first time we succeeded in obtaining the photon spectrum, keeping the balance of the total excitation energy of the ^{158}Gd nucleus (fig. 4).

Basing on the obtained data with use of the library JENDL-3.3 of the radiation capture cross-sections, elastic and inelastic neutron scattering on the nuclei of all nuclides in the natural mixture of gadolinium isotopes, the energy dependence of specific neutron kerma for natural Gd was calculated. Thus, data on the energy dependence of neutron kerma for all elements included in soft biological tissue and drugs for NCT were obtained. The following figure presents the specified dependences required for the dose calculation.

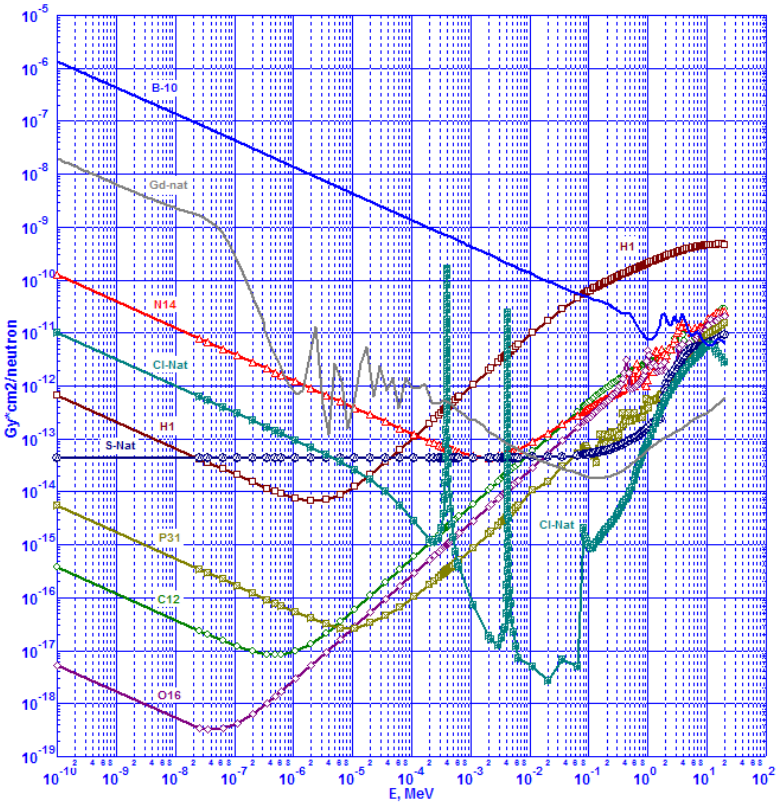

Fig. 5. Energy dependence of specific neutron kerma for the elements in biological tissue and neutron capture agents.

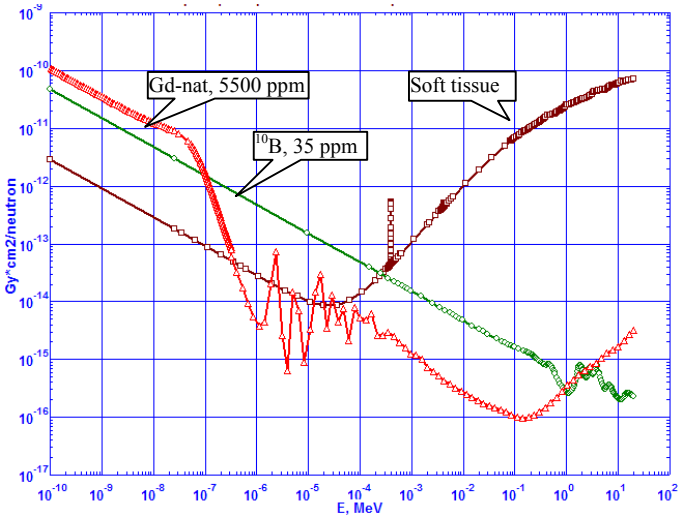

Fig. 6. Energy dependence of specific neutron kerma for biological tissue (the composition of elements corresponds to soft biological tissue) and neutron capture agents for their typical concentrations in biological tissue.

The calculated estimation of the energy dependence of specific neutron kerma for soft biological tissue in comparison with the same data for neutron capture agents at a concentration of ^{10}B - 35 ppm and Gd - 5500 ppm is given in fig. 6.

The presented data show that extra energy release in biological tissue due to gadolinium and boron can vary essentially depending on the working neutron spectrum in the range of energies < 1 eV.

Photon kerma

The energy dependence of specific photon kerma of the nuclides included in the biotissue and the drugs was calculated using the data on mass coefficients of energy absorption (μ_{en}/ρ) J.H.Hubbell, and S.M.Seltzer, from the site: http://physics.nist.gov/PhysRefData/XrayMassCoef/ of the American National Standards Institute.

The energy dependence of photon kerma factors was calculated by the expression:

$$k_i(E_\gamma) = k_D \cdot E_\gamma \times \left[\mu_{en}(E_\gamma) \Big/ \rho \right]_i, \quad Gy \cdot cm^2/photon$$

Results of the calculations are shown in fig. 7.

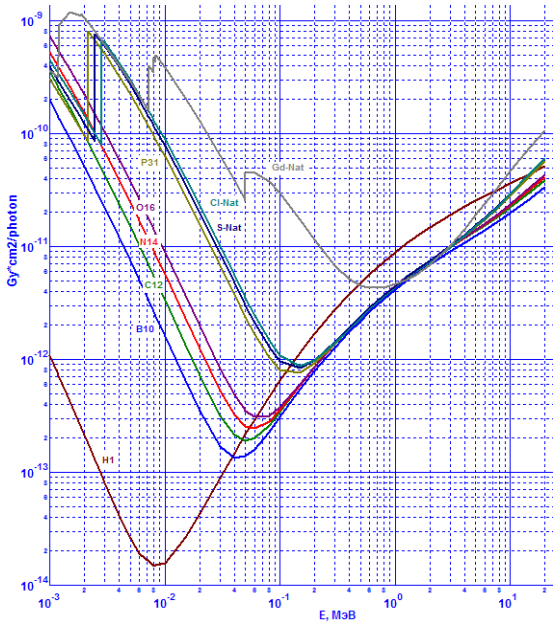

Fig. 7. Energy dependence of specific photon kerma for the basic elements of biological tissue and drugs.

Table 3

Limits of the neutron energy groups in the cross-section library BLIB2815

Group No	E_{down}, MeV	E_{up}, MeV
1	1.4000E+01	1.4500E+01
2	1.0500E+01	1.4000E+01
3	6.5000E+00	1.0500E+01
4	4.0000E+00	6.5000E+00
5	2.5000E+00	4.0000E+00
6	1.4000E+00	2.5000E+00
7	8.0000E-01	1.4000E+00
8	4.0000E-01	8.0000E-01
9	2.0000E-01	4.0000E-01
10	1.0000E-01	2.0000E-01
11	4.6500E-02	1.0000E-01
12	2.1500E-02	4.6500E-02
13	1.0000E-02	2.1500E-02
14	4.6500E-03	1.0000E-02
15	2.1500E-03	4.6500E-03
16	1.0000E-03	2.1500E-03
17	4.6500E-04	1.0000E-03
18	2.1500E-04	4.6500E-04
19	1.0000E-04	2.1500E-04
20	4.6500E-05	1.0000E-04
21	2.1500E-05	4.6500E-05
22	1.0000E-05	2.1500E-05
23	4.6500E-06	1.0000E-05
24	2.1500E-06	4.6500E-06
25	1.0000E-06	2.1500E-06
26	4.6500E-07	1.0000E-06
27	2.1500E-07	4.6500E-07
28	1.0000E-10	2.1500E-07

Phantom investigations

Studies on calculation of dose fields in a tissue-equivalent phantom (see Fig. 8) were carried out using the code RADUGA [9-11] with the library BLIB2815 (see Table 3) from the system of constants GNDL [12].

The monodirectional beam of neutrons and photons of the renovated channel HEC-4 of 6 cm in diameter on the IRT MEPhI reactor was used as a source. For neutrons, we used group approximation of the measured neutron spectrum described in [13] (see Fig.9). For photons, data on the spectrum shape calculated [13] using the code MCNP (Fig. 10) were used, which then were renormalized so that the photon dose rate in the beam would be equal to the average value of this

parameter in the series of measurements during the period of preclinical studies in 2004, = 0.25 ± 0.06 mGy/s.

The program and system of group cross-sections were tested by comparing with the results of experimental studies on the distribution of the thermal neutron flux and photon dose along the axis of the aqueous phantom of 20 cm in diameter and 32.5 cm long irradiated on the face side on the channel HEC-4 of the IRT MEPhI reactor. Beam diameter = 6 cm.

Results of the calculations and experiments are given in Fig. 11.

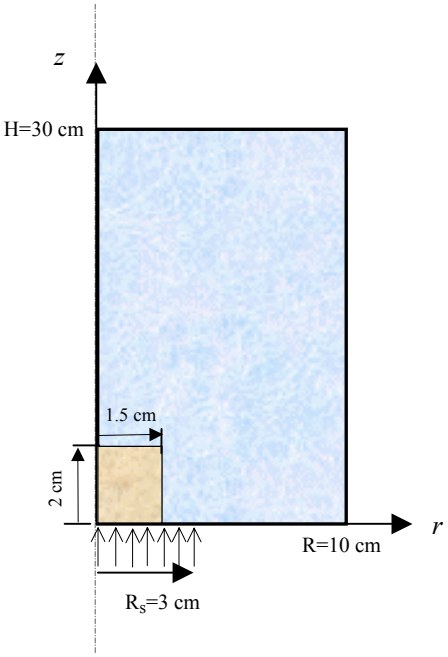

Fig.8. Cylindrical phantom with a tumor model.

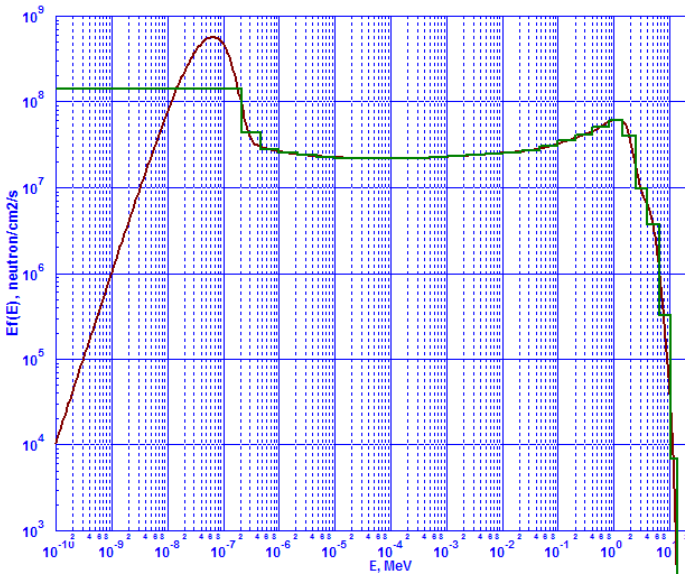

Fig. 9. Neutron spectrum of the renovated channel HEC-4 of the IRT MEPhI reactor, and its group approximation.

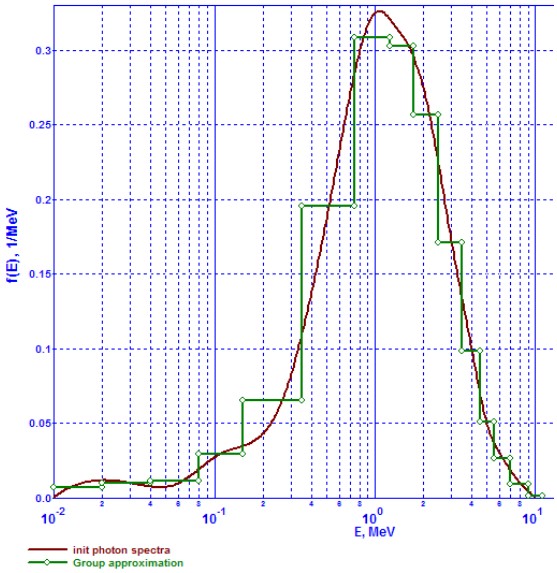

Fig. 10. Calculated photon spectrum of the channel HEC-4 of the IRT MEPhI reactor, and its group approximation. Normalized per 1 photon/s.

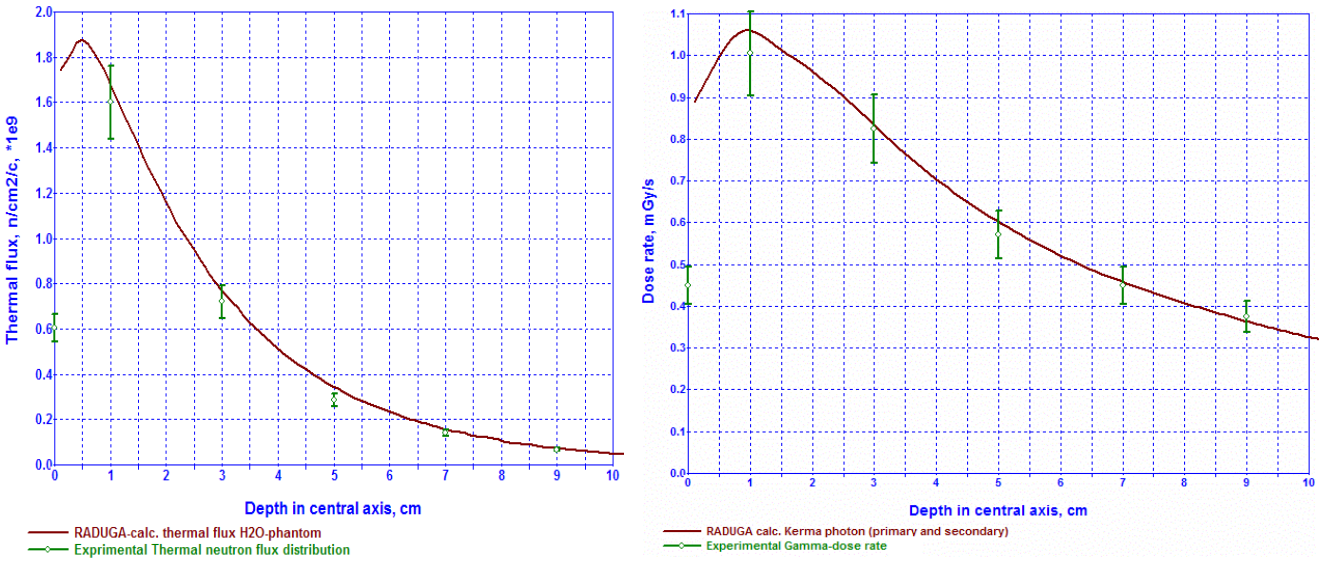

a) b)

Fig. 11. Thermal neutron flux distribution (a) and dose rates of primary and secondary gamma-radiation (b) along the axis of the aqueous phantom, calculated using the code RADUGA-5 and experimentally obtained.

The results of the calculations and experiments are in good agreement except the points on the face of the phantom.

The estimation of the neutron dose distribution in the phantom calculated using the code RADUGA-5 with the available system of group cross-sections is concerned with considerable uncertainty of the choice of group-averaged kerma factors in the thermal neutron energy region. In the cross-section library used, this energy region is described by two energy groups (see Table 3), whereas the values of kerma factors vary by 1.5 orders of magnitude (Fig. 5).

Calculation of the neutron kerma as a group approximation follows from the expression:

$$K(r) = \int dE\, \Psi(r,E) \cdot K(E) = \int dE\, \Psi(r,E) \sum_i w_i(r) k_i(E) =$$

$$= \sum_i w_i(r) \int dE \Psi(r,E) k_i(E) \approx \sum_i w_i(r) \sum_{q=1}^{Q} \Psi^q(r) k_i^{\,q}(r)$$

where $\Psi^q(r) = \int\limits_{\Delta E^q} dE \cdot \Psi(r,E)$ - neutron flux in group q, resulting from a multigroup calculation; $k_i^{\,q}(r) = \dfrac{\int\limits_{\Delta E^q} dE \cdot \Psi(r,E) \cdot k_i(E)}{\int\limits_{\Delta E^q} dE \cdot \Psi(r,E)}$ - group-averaged value of specific partial kerma; $\Psi(r,E)$ – in-group spectrum used for averaging.

The in-group spectrum was estimated by calculating the neutron flux in tissue in one-dimensional geometry using the library of neutron (27 groups) and gamma (18 groups) constants included in the applied software system SCALE-4.3 [14]. This system uses seven groups for energies < 0.4 eV (Table 4).

Table 3.10

Limits of the neutron energy groups in the group cross-section library SCALE-4.3

Group No	E lower., MeV	E up, MeV
1	6.43E+00	2.00E+01
2	3.00E+00	6.43E+00
3	1.85E+00	3.00E+00
4	1.40E+00	1.85E+00
5	9.00E-01	1.40E+00
6	4.00E-01	9.00E-01
7	1.00E-01	4.00E-01
8	1.70E-02	1.00E-01
9	3.00E-03	1.70E-02
10	5.50E-04	3.00E-03
11	1.00E-04	5.50E-04
12	3.00E-05	1.00E-04
13	1.00E-05	3.00E-05
14	3.05E-06	1.00E-05
15	1.77E-06	3.05E-06
16	1.30E-06	1.77E-06
17	1.13E-06	1.30E-06
18	1.00E-06	1.13E-06
19	8.00E-07	1.00E-06
20	4.00E-07	8.00E-07
21	3.25E-07	4.00E-07
22	2.25E-07	3.25E-07
23	1.00E-07	2.25E-07
24	5.00E-08	1.00E-07
25	3.00E-08	5.00E-08
26	1.00E-08	3.00E-08
27	1.00E-10	1.00E-08

The aforementioned constant system allowed to calculate the spatial change of the neutron spectrum, which later was used to obtain group-averaged values of partial kerma. Predictably, this dependence for the thermal neutron group of the constant system BLIB2815 appeared essential (see figure below).

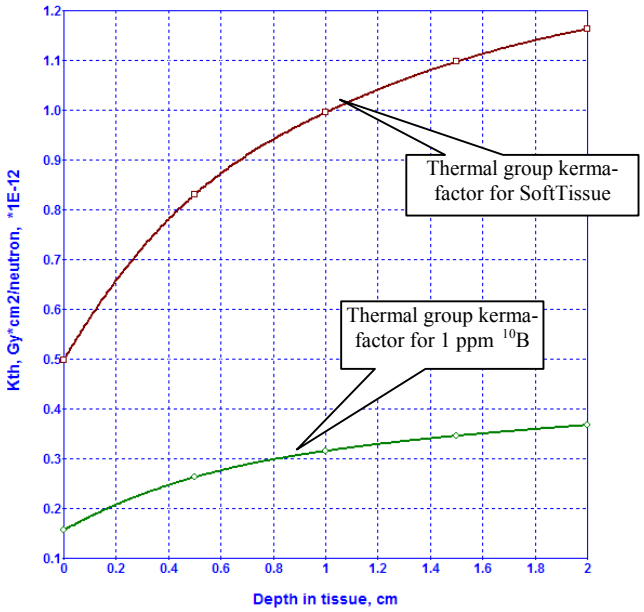

Fig. 12. Thermal group kerma factor vs. depth from the surface of the phantom.

For other groups, this dependence proved to be inessential.

Taking into account the specified method of obtaining group-averaged values of specific partial kerma, distribution of the neutron dose in the tissue-equivalent phantom was calculated; the result is shown in Fig. 13.

The calculated thermal neutron flux distributions and dose rates of neutrons and photons are given in the following figure.

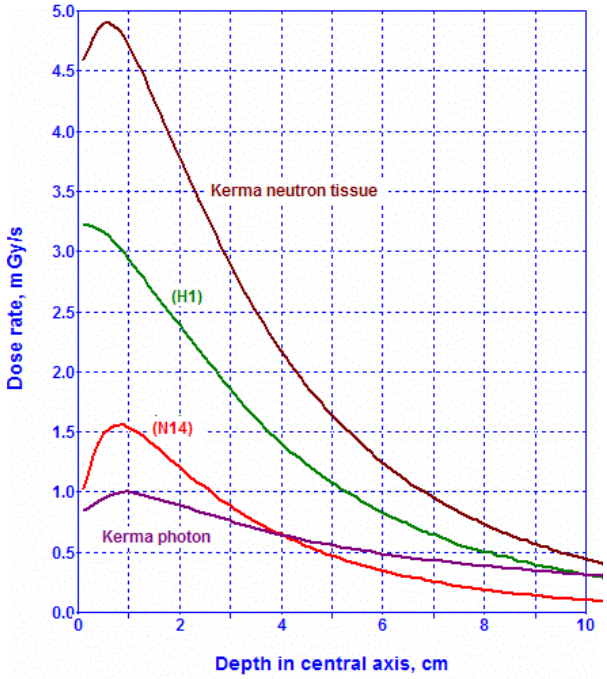

Fig. 13. Distribution of the dose rate along the axis of a homogeneous tissue-equivalent phantom, and its basic components.

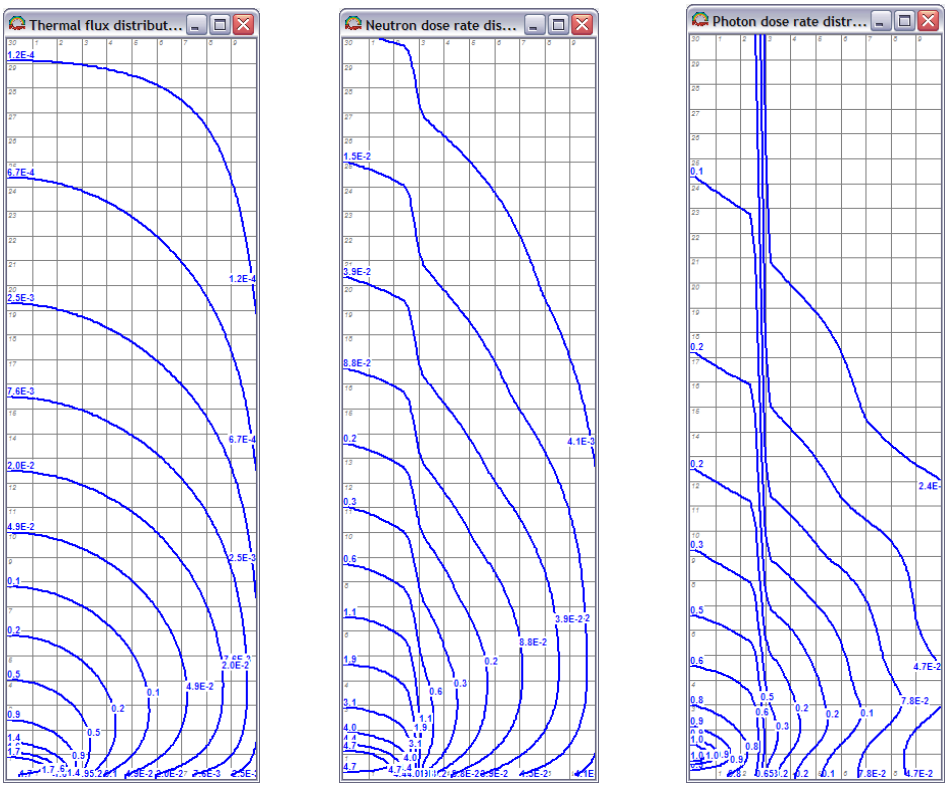

a) b) c)

*Fig. 14. Charts of distributions: a) - thermal neutron flux, neutron/cm^2/s *10^9; b) - neutron dose rate, mGy/s; c) - photons dose rate (primary and secondary), mGy/s, over the volume of the homogeneous tissue-equivalent phantom during its irradiation in the beam of the renovated channel HEC-4 of the IRT MEPhI reactor. Beam diameter = 6 cm.*

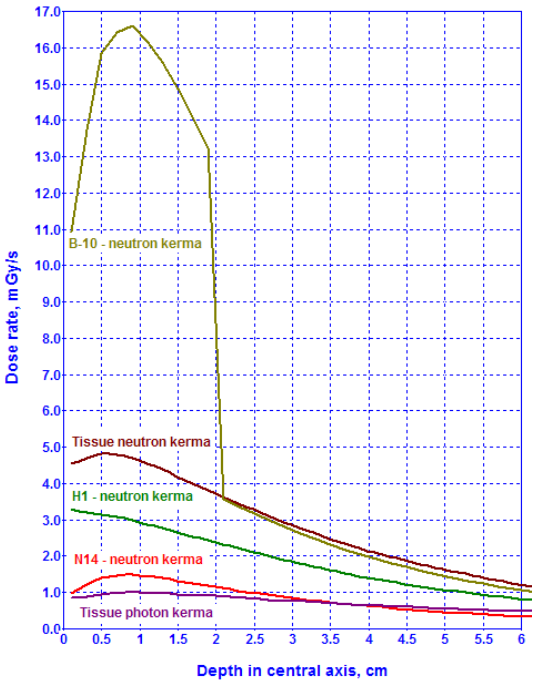

Fig. 15. Distribution of the dose rate along the axis of the tissue-equivalent phantom with a tumor model (concentration of ^{10}B in tumor - 35 ppm, in the rest of the tissue - 10 ppm), and its basic component. Calculation by the code RADUGA-5.

The estimation of the distribution of the dose components in the tissue-equivalent phantom with a tumor model containing 35 ppm of ^{10}B (the rest of the tissue contained 10 ppm of ^{10}B) is presented in Fig. 15.

Table 5 shows the values of partial components of the dose rate in soft biological tissue at various depths.

Using these data, it is possible to calculate the value of the total dose rate depending on the B-10 concentration ($\rho_{B\text{-}10}$) in the tissue:

$$D_{\Sigma}(\rho_{B-10}) = D_{tissue}^{neutron} + D_{tissue}^{photon} + \rho_{B-10} \cdot D_{1\,ppm\,B-10}\,.$$

Fig. 16 shows the values of the total dose rate depending on the B-10 concentration in the tissue calculated by the formula above.

As follows from these data, the dose on the tumor during the 1.5-hour irradiation without the drug is 29 ± 2 Gy. Taking into account the expected ^{10}B concentration in tumor ≈ 20 ppm, the dose on the tumor will be 69 ± 9 Gy.

Table 5.Dose rate of kerma components at various depths in biological tissue, Gy/min

Kerma components	Depth, cm			
	0	0.5	1.0	1.5
H-1 neutron	0.198	0.189	0.173	0.159
N-14 neutron	0.059	0.085	0.087	0.0796
H-1 + N-14 neutron	*0.257*	*0.274*	*0.26*	*0.239*
Tissue neutron, $D_{tissue}^{neutron}$	0.272	0.289	0.273	0.252
Tissue photons, D_{tissue}^{photon}	0.051	0.0568	0.0595	0.0569
$D_{tissue}^{neutron} + D_{tissue}^{photon}$	*0.323*	*0.346*	*0.333*	*0.309*
B-10 for 1 ppm, $D_{1\,ppm\,B-10}$	0.0187	0.0271	0.0277	0.0255

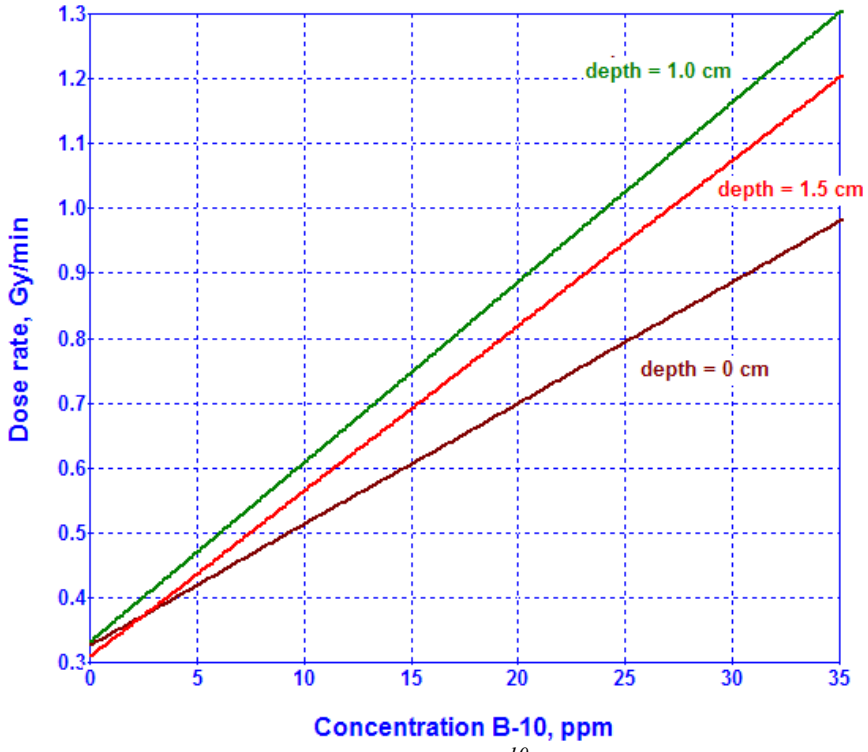

Fig. 16. Dose rate at various depths vs ^{10}B concentration in biological tissue.

Conclusion

The data presented here are the basis for the treatment planning for experimental animals in the preclinical studies on neutron capture therapy on the channel HEC-4 of the IRT MEPhI nuclear reactor.

The work is carried out with financial support ISTC, Project # 1951.

References

1. J.T. Goorley, W.S. Kiger III, and R.G. Zamenhof, "Reference Dosimetry Calculations for Neutron Capture Therapy with Comparison of Analytical and Voxel Models," Medical Physics, vol. 29 No. 2, February 2002, p. 145-156.
2. J. Stepanek, Radiation spectrum of ^{158}Gd and radial dose distribution. In Advances in Neutron Capture Therapy 2 (B. Larsson, J. Crawford and R. Weinreich, Eds.). Excerpta Medica, Int. Cong. Series 1132, Elsevier, Amsterdam, 1997.
3. C. K. C Wang, M. Sutton, T. M. Evans and B. H. Laster, A microdosimetric study of $^{10}B(n,\alpha)^{7}Li$ and $1^{57}Gd(n,\gamma)$ reactions for neutron capture therapy. In Proceedings of the Sixth International Radiopharmaceutical Dosimetry Symposium (A. T. Stelsen, M. G. Stabin and R. B. Sparks, Eds.), pp. 336–344. Report ORISE 99-0164, Oak Ridge Institute for Science and Education, Oak Ridge, TN, 1999.
4. Tim Goorley, Hooshang Nikjoo, Electron and Photon Spectra for Three Gadolinium-Based Cancer Therapy Approaches. Radiat. Res. 54, 556–563 (2000).
5. J. K. Tuli, Evaluated Nuclear Data File. Report BNL-NCS-51655-Rev. 87, Brookhaven National Laboratory, Upton, NY, 1987.
6. L.V.Groshev, A.M.Demidov, V.N.Lutsenko, V.I.Pelekhov, Atlas of gamma spectra of the thermal neutron capture. – M: Atomizdat,1958. - 111 p.
7. S.A.Klykov, S.P.Kapchigashev, V.I.Potetnya et al. Experimental determination of energy release in the neutron capture by gadolinium. Atomnaya Energiya, v.91, i.6, December 2001.
8. Y.Sakurai, T.Kobayashi. Experimental Verification of the Nuclear Data of Gadolinium for Neutron Capture Therapy. Journal of NUCLEAR SCIENCE and TECHNOLOGY, Supplement 2, p. 1294-1297 (August 2002).
9. L. P. Bass, A. N. Goncharov et al., “RADUGA-4.0 - Two-Dimensional Transport Code, ” *Proc. Int. Topical Meeting on Advances in Mathematics, Computations and Reactor Physics*, April 28 - May 2, 1991, Pittsburgh, USA,., vol. 5, p. 30.3 7-1
10. *L.P.Bass, O.V.Nikolaeva.* Raduga-5 - the code to solve the transport equation in 2D and 3D geometries. // Proceedings "Neutronics–99" of the seminar " Algorithms and software for neutronic calculations of nuclear reactors". Obninsk. 26–28 October 1999. p. 145–149.
11. The code Raduga-5.1 (P) for the solution of the transport equation in 2D and 3D geometries on computers with parallel architecture. User manual. Report of Keldysh IAM RAS, 2002.
12. A. V. Voronkov, S. A. Gayfulin, V. I. Zhuravlev et. al., “GNDL - Program System of Group Constants to Provide Calculations of Neutron and Photon Fields,” Proc. Int. Topical Meeting on Advances in Mathematics, Computations and Reactor Physics, April 28 - May 2, 1991, Pittsburgh, USA, vol. 5, p. 30.5 2-1.
13. *E.I.Grigor'ev et al.* Physical characteristics of the horizontal NCT beam's of IRT MIPhI (rus.), In; Scientific session MIPhI, v.**5**. Medical Physics, Biophysics, M., p. 26 (2003).
14. “SCALE 4.3 – Modular Code System for Performing Standardized Computer Analyses for Licensing Evaluation for Workstations and Personal Computers”, Radiation Shielding Information Computational Center, CCC-545 (1997).